Low-noise visible-blind photodetectors based on $SrTiO_3$ single crystal with transparent indium tin oxide electrode as window

Er-Jia Guo,[1] Hui-Bin Lu,[1,*] Meng He,[1] Jie Xing,[1,2] Kui-Juan Jin,[1] and Guo-Zhen Yang[1]

[1]Beijing National Laboratory for Condensed Matter Physics, Institute of Physics, Chinese Academy of Sciences, Beijing 100190, China

[2]School of Materials Sciences and Technology, China University of Geosciences, Beijing 100083, China

*Corresponding author: hblu@aphy.iphy.ac.cn

Received 4 February 2010; accepted 15 March 2010; posted 16 March 2010 (Doc. ID 123817); published 4 May 2010

We fabricate low-noise visible-blind ultraviolet photodetectors of indium tin oxide/$SrTiO_3$/Ag (ITO/STO/Ag) based on the properties of STO bandgap excitation and the conductance of ITO thin film. The ITO films are epitaxially grown on STO wafers as electrodes and windows of the photodetectors, simultaneously. The photodetectors have low noise and very good electromagnetic shielding. The dark current is as low as 270 pA even at a 200 V bias. The peak responsivity reaches to 30 mA/W at the wavelength of 360 nm. From the experimental results, the same ideas can be generalized to develop visible-blind and solar-blind UV photodetectors based on wide bandgap materials, such as $LaAlO_3$, $LiNbO_3$, $LiTaO_3$, $BaTiO_3$, ZnO, MgO, and ZrO_2. © 2010 Optical Society of America

OCIS codes: 040.5160, 040.5150, 040.7190, 310.7005.

1. Introduction

Ultraviolet (UV) light detection has drawn a great deal of interest in recent years due to many civil and military requirements, such as fire forecasting, secure communication, and environmental detection [1–3]. In particular, UV detection with high discrimination against visible and infrared light is ideal for detection under the background of visible and infrared radiation. Although traditional semiconductors, including Si and GaAs, can be used in UV detection, they need external filters to block visible and infrared light due to their long wavelength response. Some groups have reported UV photodetectors based on wide bandgap materials, including III–V nitrides [4,5], *c*BN [6], ZnO [7], and diamond [8]. However, the UV photodetectors require a complicated fabrication process and high-cost manufacture. Recently, we reported visible-blind or solar-blind UV photodetectors based on the perovskite oxide single crystals with wide bandgap, including $SrTiO_3$ (STO) [9,10], $LaAlO_3$ [11], $LiNbO_3$ [12], and $LiTaO_3$ [13], with Au interdigitated electrodes. Photodetectors based on the perovskite oxide single crystals have high sensitivities and low dark currents; however, practical devices must have anti-interference abilities. There are some problems with the structure of interdigitated electrodes. One problem is that the anti-interference is not good enough for electromagnetic interferences. Another problem is contaminants, such as the dusts or particles, in the air. Contaminants with conductive particles may lead to short circuits between interdigitated electrodes so that photodetectors cannot work well. In this paper, we report the low-noise visible-blind UV photodetectors of indium tin oxide (ITO)/STO/Ag based on the properties of STO bandgap excitation and the conductance of ITO thin film.

0003-6935/10/142557-04$15.00/0

2. Experimental Details

Indium tin oxide thin films as transparent electrodes have been widely used in panel displays, solar cells, and optoelectronics due to ITO's low electrical resistivity and high transparency [14–16]. Figure 1 shows the schematic diagram of the ITO/STO/Ag photodetectors. ITO thin film is epitaxially grown on a surface of STO as an electrode and window. The ITO thin film is connected in the cavity with Ag glue as a function of electromagnetic interference. The other surface of STO is smeared with Ag glue uniformly as another electrode. Because the ITO film has a good metallike property, the detector chip is a metal(ITO)-insulator (STO)-metal(Ag) (MIM) structure. The detector chip and the sampling resistance R are installed in a Cu cavity, so the photodetector has low noise and a very good electromagnetic shield. The mechanism of photocurrent is similar to STO photodetectors with interdigitated electrodes [10] and can be understood as following: the incident light passes through the ITO film and into the STO single crystal, STO absorbs the incident photons and generates the photocarriers (electrons and holes). The photogenerated electrons and holes are separated by the electric field of the supplied bias and then form the photocurrent. We have proved that the cutoff wavelength of a STO single crystal is at about 390 nm, corresponding to 3.2 eV of STO bandgap [9,10]. The photoelectric process in STO is a bandgap excitation process, which indicates that the device has an intrinsic characteristic of visible blindness.

The STO wafers used in the present study are as-supplied commercial STO single crystals with a purity of 99.99% and are mirror polished. The geometry of STO wafers is 5 mm × 10 mm with a thickness of 0.5 mm. We epitaxially grow ITO thin films on the STO wafers by a laser molecular-beam epitaxy system [17]. The preparation conditions of the ITO films are as follows: a sintered ceramic ITO target (In_2O_3:SnO_2 = 90:10 wt.%) is used in our experiment; the laser beam has a wavelength of 308 nm, a repetition rate of 2 Hz, and a duration of 25 ns; the energy density was approximately 1.5 J/cm^2; the temperature of the STO wafers was kept at 680 °C; and oxygen pressure of 1.5×10^{-1} Pa was maintained throughout the deposition. ITO films with thicknesses of 10, 20, 50, and 200 nm were deposited on the STO wafers. The thicknesses of the ITO films are controlled by the intensity oscillations of *in situ* reflection high-energy electron diffraction (RHEED) and further confirmed by a surface profile measuring system.

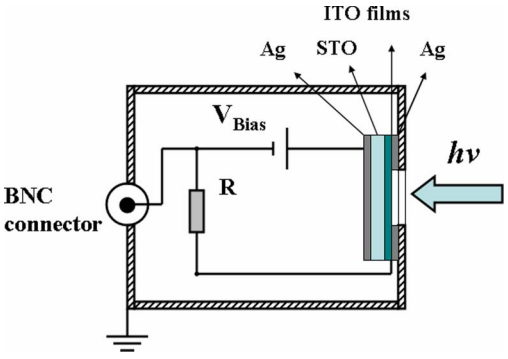

Fig. 1. (Color online) Schematic diagram of ITO/STO/Ag photodetector.

3. Results and Discussion

Figure 2 presents a typical x-ray diffraction (XRD) $\theta - 2\theta$ scan curve of a 200 nm ITO film on STO substrate. Except for ITO (00l) and STO (00l) diffraction peaks, there is no other diffraction peak from impurity phases or randomly oriented grains. The RHEED pattern of 200 nm ITO film is shown in the inset of Fig. 2. The results of *in situ* RHEED and *ex situ* XRD in Fig. 2 indicate that the ITO film is single phased and epitaxially grown on the STO substrate. The Hall measurement confirmed that the resistivities of the ITO films are 1.16×10^{-2}, 2.75×10^{-3}, 4.32×10^{-4}, and $8.68 \times 10^{-5}\ \Omega \cdot$cm, for 10, 20, 50, and 200 nm films, respectively. The carrier densities of all the ITO films are over the level of 10^{20} cm^{-3}. To our knowledge, the resistivities are the smallest resistivities reported up to now for ITO films with the same thicknesses.

To obtain the optimal MIM structure, we polished three pieces of STO with 10 nm ITO films mechanically, and let the thicknesses decrease to 0.1, 0.18, and 0.25 mm. We studied the influences of the thicknesses of the ITO film and the STO single crystal on the photoelectric sensitivity. As shown in Fig. 1, the diameter of the detection window is 4 mm, and the effective area of the photodetectors is 12.56 mm^2. A tunable DC voltage source is taken as the applied bias. The photovoltage signals taken from a sampling resistance R are recorded by a digital voltmeter. A dome light-emitting diode (LED) with a wavelength of 365 nm and an Hg lamp (253.65 nm) are employed as the light sources. The light intensities are calibrated by a UV-enhanced photodetector in the wavelength range of 200–500 nm.

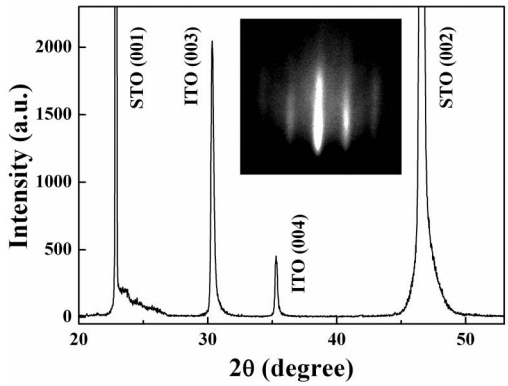

Fig. 2. Typical XRD $\theta - 2\theta$ scan curve of a 200 nm ITO film on STO substrate. The inset shows a RHEED pattern of a 200 nm ITO film after deposition.

Figure 3(a) shows the bias dependence of the photocurrent responsivities for the three photodetectors with 10 nm thick ITO film and different STO thickness of 0.1, 0.18, and 0.25 mm under the irradiation of 365 nm light, respectively. The photocurrent responsivities increase linearly with applied bias for all three photodetectors. The responsivities increase rapidly with the decrease of STO thickness, and the maximum responsivities of a photodetector with a 0.1 mm STO reaches 14 and 29 mA/W at 100 and 200 V bias, respectively. It is easy to understand that the thinner STO wafer has the larger electrical field under the same applied bias, so the responsivity of photodetector with a thinner STO is higher than that with a thicker STO. After carefully fitting the experimental data, we got a relationship of photocurrent of $\propto t^{-2}$, where t is the thickness of the STO wafer. This agrees well with the theory of photoconductive detectors [18,19].

Figure 3(b) presents the photocurrents varying with power density for the same three photodetectors and measurement conditions as Fig. 3(a). The photocurrents also present a good linear relationship with the power density for all the three photodetectors, and the responsivities increase with the decrease of STO thickness. The inset of Fig. 3(b) shows the photocurrents varying with power densities for a photodetector with a 0.1 mm STO under the illumination of a weak light. The photodetector can detect UV light as low as 3.4 nW or even more smaller, indicating that the photodetectors have a high responsivity.

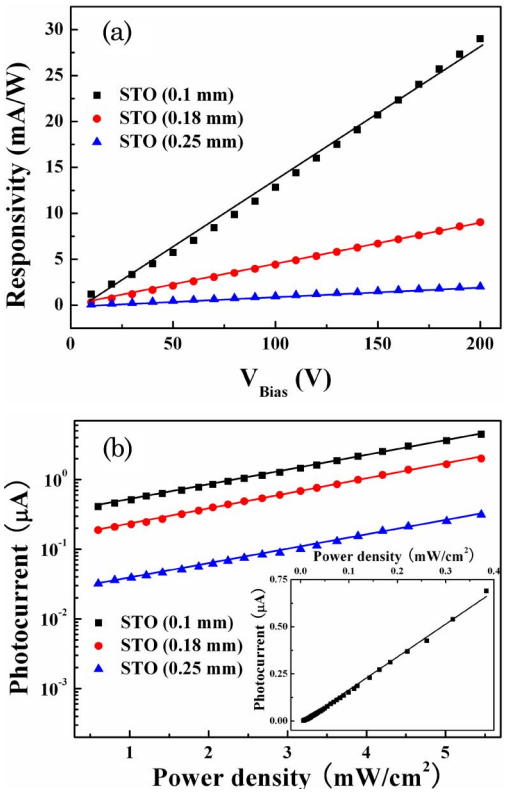

Fig. 3. (Color online) (a) Bias dependence of the photocurrent responsivities for the photodetectors with 10 nm thick ITO film and different thicknesses of STO under irradiation of 365 nm light. (b) Photocurrent variation with incident power density with the same three photodetectors and experimental conditions in (a). The inset shows the photocurrent variation with power density for a photodetector with 0.1 mm STO and 10 nm ITO under very weak light.

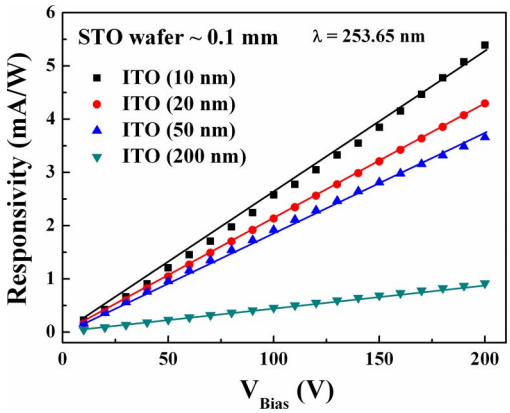

Fig. 4. (Color online) Bias dependence of the photocurrent responsivities for the photodetectors with 0.1 mm thick STO and different thicknesses of ITO under Hg lamp irradiation.

We further studied the influences of the thickness of ITO films on the responsivity of photodetectors with 0.1 mm STO and different ITO thickness of 10, 20, 50, and 200 nm using an Hg lamp (253.65 nm). Figure 4 exhibits the photocurrent responsivity of photodetectors as a function of the applied bias under Hg lamp illumination. The photocurrent responsivities increase linearly with applied bias for all the three photodetectors. It is obvious that the responsivities increase rapidly with the decrease of ITO thickness. The results indicate that, despite the ITO thin films having the advantage of high conductivity, the absorption of UV light is a disadvantage for UV photodetectors because the bandgap of ITO is ~4 eV [16]. To improve the responsivity of detectors, it is suitable to choose the thinner ITO film as the electrode.

The spectral response is measured using a 30 W D_2 lamp as a light source and a monochromator combined with an optical chopper and a lock-in amplifier.

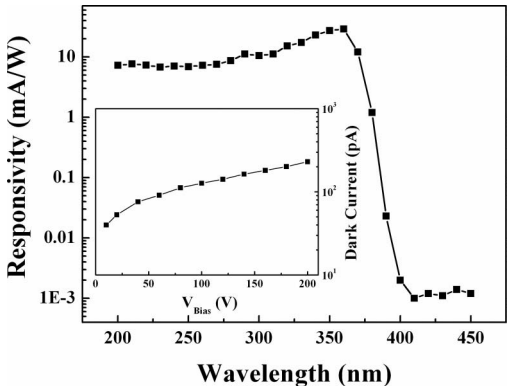

Fig. 5. Spectral response of a photodetector with 0.1 mm STO and 10 nm ITO. The inset shows the dark currents varying with the external applied bias.

Figure 5 shows the spectrum response of a photodetector with 0.1 mm STO and 10 nm ITO film at 200 V bias. The wavelength of the peak response is at 360 nm, and the photocurrent responsivity is about 30 mA/W. The quantum efficiency η is calculated to be 10.3% according to the formula $\eta = R_i h\upsilon/q$, where R_i is the responsivity of the photodetector, h is the Planck constant, υ is the frequency of incident light, and q is the electronic charge. The cutoff wavelength is at about 390 nm, which is in agreement with the absorption spectrum of STO single crystals [9]. The UV/visible contrast ratio is over 3 orders of magnitude, indicating that the photodetector has intrinsic visible blindness. The bias dependence of the dark current is shown in the inset of Fig. 5 for a photodetector with a 0.1 mm STO and 10 nm ITO film. The dark currents are only 40, 76, 127, and 270 pA at 10, 40, 100, and 200 V, respectively, because the STO single crystal is an intrinsic insulator without UV light illumination.

4. Conclusions

We have designed and successfully fabricated a low-noise visible-blind MIM UV photodetector based on the properties of STO bandgap excitation and the conductance of ITO thin film. The dark current is as low as 270 pA even at a 200 V bias. The photodetector has a high responsivity and can detect UV light at 3.4 nW or even smaller. The responsivity and quantum efficiency are not higher than those of a STO single crystal with interdigitated electrodes, as we reported previously [10]; however, from the point of view of application, the MIM structure photodetectors have many potential applications in UV detection due to the low noise and adequate responsivity. In addition, the responsivity can be improved greatly by, for example, further decreasing the thickness of the STO or replacing the STO single crystal with STO thin films. Furthermore, the ideas can be generalized to develop new visible-blind and solar-blind UV photodetectors with wide bandgap materials, such as $LaAlO_3$, $LiNbO_3$, $LiTaO_3$, $BaTiO_3$, ZnO, MgO, and ZrO_2.

This work is supported by the National Basic Research Program of China and the National Natural Science Foundation of China (NSFC).

References

1. A. Osinsky, S. Gangopadhyay, B. W. Lim, M. Z. Anwar, M. A. Khan, D. V. Kuksenkov, and H. Temkin, "Schottky barrier photodetectors based on AlGaN," Appl. Phys. Lett. **72**, 742–744 (1998).
2. T. Tut, T. Yelboga, E. Ulker, and E. Ozbay, "Solar-blind AlGaN-based *p-i-n* photodetectors with high breakdown voltage and detectivity," Appl. Phys. Lett. **92**, 103502 (2008).
3. H. Jiang and T. Egawa, "High quality AlGaN solar-blind Schottky photodiodes fabricated on AIN/sapphire template," Appl. Phys. Lett. **90**, 121121 (2007).
4. E. Muñoz, E. Monroy, J. A. Garrido, I. Izpura, F. J. Sánchez, M. A. Sánchez-García, E. Calleja, B. Beaumont, and P. Gibart, "Photoconductor gain mechanisms in GaN ultraviolet detectors," Appl. Phys. Lett. **71**, 870–872 (1997).
5. M. Mikulics, M. Marso, P. Javorka, P. Kordo, and H. Lüth, "Ultrafast metal-semiconductor-metal photodetectors on low-temperature-grown GaN," Appl. Phys. Lett. **86**, 211110 (2005).
6. A. Soltani, H. A. Barkad, M. Mattalah, B. Benbakhti, J.-C. De Jaeger, Y. M. Chong, Y. S. Zou, W. J. Zhang, S. T. Lee, A. BenMoussa, B. Giordanengo, and J.-F. Hochedez, "193 nm deep-ultraviolet solar-blind cubic boron nitride based photodetectors," Appl. Phys. Lett. **92**, 053501 (2008).
7. P. Sharma, K. Sreenivas, and K. V. Rao, "Analysis of ultraviolet photoconductivity in ZnO films prepared by unbalanced magnetron sputtering," J. Appl. Phys. **93**, 3963–3970 (2003).
8. A. Balducci, M. Marinelli, E. Milani, M. E. Morgada, A. Tucciarone, and G. Verona-Rinati, "Extreme ultraviolet single-crystal diamond detectors by chemical vapor deposition," Appl. Phys. Lett. **86**, 193509 (2005).
9. K. Zhao, K. J. Jin, Y. H. Huang, S. Q. Zhao, H. B. Lu, M. He, Z. H. Chen, Y. L. Zhou, and G. Z. Yang, "Ultraviolet fast-response photoelectric effect in tilted orientation $SrTiO_3$ single crystals," Appl. Phys. Lett. **89**, 173507 (2006).
10. J. Xing, K. Zhao, H. B. Lu, X. Wang, G. Z. Liu, K. J. Jin, M. He, C. C. Wang, and G. Z. Yang, "Visible-blind, ultraviolet-sensitive photodetector based on $SrTiO_3$ single crystal," Opt. Lett. **32**, 2526–2528 (2007).
11. J. Xing, E. J. Guo, K. J. Jin, H. B. Lu, J. Wen, and G. Z. Yang, "Solar-blind deep-ultraviolet photodetectors based on an $LaAlO_3$ single crystal," Opt. Lett. **34**, 1675–1677 (2009).
12. E. J. Guo, J. Xing, K. J. Jin, H. B. Lu, J. Wen, and G. Z. Yang, "Photoelectric effects of ultraviolet fast response and high sensitivity in $LiNbO_3$ single crystal," J. Appl. Phys. **106**, 023114 (2009).
13. E. J. Guo, J. Xing, H. B. Lu, K. J. Jin, J. Wen, and G. Z. Yang, "Ultraviolet fast-response photoelectric effects in $LiTaO_3$ single crystal," J. Phys. D **43**, 015402 (2010).
14. Y. Z. Chiou and J. J. Tang, "GaN photodetectors with transparent indium tin oxide electrodes," Jpn. J. Appl. Phys. **43**, 4146–4149 (2004).
15. M. L. Lee, P. F. Chi, and J. K. Sheu, "Photodetectors formed by an indium tin oxide/zinc oxide/p-type gallium nitride heterojunction with high ultraviolet-to-visible rejection ratio," Appl. Phys. Lett. **94**, 013512 (2009).
16. W. S. Jahng, A. H. Francis, H. Moon, J. I. Nanos, and M. D. Curtis, "Is indium tin oxide a suitable electrode in organic solar cells? Photovoltaic properties of interfaces in organic p/n junction photodiodes," Appl. Phys. Lett. **88**, 093504 (2006).
17. G. Z. Yang, H. B. Lu, F. Chen, T. Zhao, and Z. H. Chen, "Laser molecular beam epitaxy and characterization of perovskite oxide thin films," J. Cryst. Growth **227**, 929 (2001).
18. M. Razeghi and A. Rogalski, "Semiconductor ultraviolet detectors," J. Appl. Phys. **79**, 7433–7473 (1996).
19. T. Palacios, E. Monroy, F. Calle, and F. Omnes, "High-responsivity submicron metal-semiconductor-metal ultraviolet detectors," Appl. Phys. Lett. **81**, 1902–1904 (2002).